Supplemental Information:

This section contains:

Detailed Materials and Methods

References cited in Supplemental Materials

Detailed Materials and Methods:

Mice

Fstl3 gene deleted (FSTL3 KO) (1) and wildtype (WT) mice (C57BL/6) were maintained at 14:10 light and dark cycles. All animal studies complied with US Department of Agriculture (Protocol Number: 2005N000131/2) or UK Home Office guidelines (Project License: PPL 70/6424).

Histology and Histomorphometry

Testes were isolated from mice at different ages and fixed in 4% paraformaldehyde (for immunohistochemistry) or Bouin's fixative (for histology, histomorphometry and stereology) overnight. Tissues were then processed for paraffin embedding. Multiple 6μm-thick microtome sections from each tissue were stained with haematoxylin and eosin and photographed. For measurement of seminiferous tubule size distribution, Adobe Photoshop size measurement tools were used on microscope images to measure the shortest diameter of seminiferous tubules of circular cross-section. Obliquely sectioned tubules were excluded from analyses.

Stereology

Testes were embedded in Technovit 7100 resin, cut into 20μm sections and stained with Harris's haematoxylin. The total testis volume was estimated using the Cavalieri principle (*2*) and the same slides used to estimate the number of cells were also used to estimate testis volume. The optical dissector technique (*3*) was used to count the number of Leydig, Sertoli and germ cells in each testis.

Sertoli and germ cells were identified by their distinctive nuclei and position within the tubule while the Leydig cells were identified by their position within the interstitial tissue and by their round nuclei and prominent nucleoli as previously described (*4*). The numerical density of each cell type was estimated using an Olympus BX50 microscope fitted with a motorized stage (Prior Scientific Instruments) and Stereologer software (Systems Planning Analysis).

Immunofluorescence and Immunohistochemistry

Immunolocalisation was performed as previously described (9). Briefly, paraffin-embedded tissue sections were de-waxed in xylenes, rehydrated and antigen was retrieved with 0.01M sodium citrate buffer. The sections were then incubated in phosphate buffered saline (PBS) containing 0.1% Triton X-100 for 20 minutes, washed and incubated in 10% horse serum in PBS for 1 hour at room temperature. Sections were incubated with primary antibodies at recommended dilutions at 4°C overnight. The primary antibodies used were rabbit polyclonal antibodies against phospho-SMAD2, pSMAD2 (Millipore), AKT and SIRT1 (Cell Signaling). For double immunofluorescence using pSMAD2 (Millipore) and SIRT1 (Cell Signaling) rabbit polyclonal antibodies, the staining was performed sequentially as described before (12) - SIRT1 antibody was probed with Alexa-Fluor-594-conjugated goat anti-rabbit IgG (Invitrogen) followed by extensive washes and then incubation with pSMAD2 antibody, probed with Alexa-Fluor-488-conjugated goat anti-rabbit IgG (Invitrogen). Sections were mounted using fluorescent mounting medium (Vector) and photographed using a Leica DM4000B fluorescence microscope. Appropriate controls to address specificity of secondary antibodies, and experiments with single antibodies were also performed to ensure double immunolocalisation is not an artifact. For immunohistochemical detection, the sections were processed with an anti-rabbit Vectastain Elite ABC kit (Vector Laboratories) and NovaRed substrate kit (Vector Laboratories).

Microdensitometry (to Assess Phospho-SMAD2 Expression per Cell)

Serial 10μm sections of WT and FSTL3 KO mouse testes were immunohistochemically labelled for detection of phospho-SMAD2 as described above. Labeling intensity, a measure of expression per

cell, was measured in cells located at the periphery (early, E) and intermediate and central (late, L) zones of seminiferous tubules using a Vickers M85A scanning and integrating microdensitometer at 550nm (*5*). At least 8 cells in each zone, in multiple tubules, in each of 5 sections from WT and FSTL3 KO mouse testes were evaluated. The amount of reaction product per cell was expressed as mean integrated extinction (x100).

Flow Cytometry

Flow cytometric analyses of testicular cells were performed as described previously (6). Briefly, testes were dissected, decapsulated and incubated in 0.25mg/ml collagenase type 3 (Sigma) at 32°C for up to 30 minutes with agitation. Dispersed tubules were washed twice in PBS and then incubated with 0.25mg/ml trypsin (GibcoBRL) and 1mg/ml DN*ase*I (Sigma) at 32°C for 10 minutes with agitation. Trypsin digestion was terminated by adding an equal volume of DMEM containing 10% fetal bovine serum (DMEM/FBS). Digested tubules were collected by centrifugation and resuspended by gentle trituration in DMEM/FBS to obtain a single-cell suspension. This was filtered through a 50µm mesh (Costar), stained with trypan blue and counted in a haemocytometer. Germ cell suspensions were stained with propidium iodide (PI) for DNA content and nuclear size analysis. 2x10^{5} cells were rinsed once with balanced salt solution, resuspended in 0.2 ml of cold PI staining solution (10mM Tris, pH 8.0, 150mM NaCl, 0.1% Nonidet P40, 10 µg/ml RNaseA and 50 µg/ml PI), vortexed for 2-3 seconds and incubated on ice for 10 minutes to lyse the plasma membrane and stain nuclear DNA. Nuclear size and complexity and DNA content were determined on a BDCanto II analyser with PI detected in the phycorerythrin (PE) channel with linear amplification. The FSC and SSC profiles were gated as described before (6) to identify germ cell populations.

RNA Expression Data Mining

Gene expression omnibus (GEO) datasets were searched for gene expression during mouse spermatogenesis and the ‘Spermatogenesis and testis development time course (MG-U74B)’ dataset was selected as the primary data source. Data between two time points during testis development were

compared and significantly altered mRNA were identified using a two-tailed t-test with a significance level of $p < 0.05$. Genes expressed differentially during the time windows of 0-14, 20-35 and 20-56 days (corresponding to somatic expansion, first wave of spermatogenesis, and spermatogenesis to post-pubertal development, respectively) in comparison to the rest of the time windows were thus identified.

Testis Explant Cultures

WT mice were euthanized using CO_2 and testes were dissected using aseptic techniques. Dissected testes were de-tunicated and rapidly divided into 6 parts using sharp tweezers. These parts were briefly washed in OptiMEM containing antibiotics, gently teased to loosen tubules and cultured in OptiMEM in the presence or absence of either 25ng/ml activin (Peprotech) or 100ng/ml FSTL3 (R&D Labs) for 16 hours at 32°C. At the end of treatment, cultured testis explants were washed once in ice-cold PBS and directly lysed in lysis buffer (50mM Tris-HCl, pH 7.4, 1% NP-40, 150mM NaCl, 20mM NaF, 10mM $Na_2P_2O_7$, 1mM Na_3VO_4) supplemented with a mixture of protease inhibitors (Complete Mini, Roche Applied Science).

Preparation of Tissue Lysates and Western Blotting

Frozen tissue samples were pulverized in dry ice and homogenized in lysis buffer (50mM Tris-HCl, pH 7.4, 1% NP-40, 150mM NaCl, 20mM NaF, 10mM $Na_2P_2O_7$, 1mM Na_3VO_4) supplemented with a mixture of protease inhibitors (Complete Mini, Roche Applied Science). This homogenate was then sonicated at low power to shear chromosomal DNA and centrifuged to remove debris. Protein concentrations were estimated using a Bradford colorimetric assay (Bio-Rad). 50µg of total protein lysate were loaded on 10% SDS PAGE gels and size separated using constant current. After electrophoresis, proteins were transferred from gels to pure nitrocellulose membranes (Amersham Biosciences) and efficiency of transfer assessed by Ponceau-S staining. The membranes were then washed in TBST (50 mM Tris pH7.5, 150 mM NaCl, 0.05% Tween 20) and incubated with blocking buffer (5% non-fat dry milk in TBST) at room temperature for 1 hour. Protein blots were incubated with primary antibodies, used at recommended dilutions in blocking buffer, overnight at 4°C.

Membranes were washed three times with TBST and then incubated with appropriate horseradish peroxidise conjugated secondary antibodies (Sigma). The membranes were again washed four times and immune complexes formed on the blot were visualized by ECL (Amersham Biosciences). Immunoreactive protein bands were analyzed using the public domain NIH Image program (developed at the United States National Institutes of Health and available on the Internet at http://rsb.info.nih.gov/nih-image/). Of the AKT antibodies used in this study, pan-AKT antibody reacts to all three forms of AKT and phosphoAKT antibody identifies AKT phosphorylated at Ser473.

Quantitative Proteomics

Preparation of Lysates: Freshly dissected testes were lysed in a dounce-homogeniser in lysis buffer (50mM Tris pH 8.1, 75mM NaCl, 8M urea, 10mM sodium pyrophosphate, 1mM sodium fluoride, 1mM β-glycerophosphate, 1mM sodium orthovanadate) supplemented with a mixture of protease inhibitors (Complete Mini, Roche Applied Science). This homogenate was then sonicated at low power to shear chromosomal DNA and centrifuged to remove debris. The supernatant was collected into a new tube and protein concentration was measured using a Bradford colorimetric assay (Bio-Rad).

Sample Preparation: Reduction and alkylation of cysteines were performed on 15 mg of testis protein by incubation in 2.5mM DTT for 25 minutes at 60°C and then 30 minutes at room temperature in 7mM iodoacetamide in the dark, respectively. The alkylation reaction was quenched by the addition of DTT to 2.5mM and an additional 15 minutes incubation. Lysate was 8-fold diluted (25mM Tris, pH 8.1, 1mM $CaCl_2$), and 40 μg of sequencing grade trypsin (Promega) was added (5ng/ml trypsin; enzyme/substrate ratio of 1:250). Digestion was stopped after 16 h at 37°C by the addition of trifluoroacetic acid (TFA) to 0.4%, and the pH was verified at = 2. The digest was centrifuged at 3,200 rpm to remove insoluble material and then loaded onto a 500-mg tC18 SepPak cartridge (Waters) for peptide desalting. Eluted peptides were labeled with either normal (no isotope label) or heavy (d6), dimethyl groups for WT and FSTL3 KO respectively (*7*). Peptides from KO and WT testes were mixed, lyophilized and stored at -20°C until further use.

Liquid Chromatography Tandem Mass Spectrometry (LC-MS/MS) Analyses: Dried peptides were resuspended in 5% acetonitrile (ACN) and 4% formic acid (FA) and 2 µl was loaded onto a microcapillary column packed with C18 beads (Magic C18AQ, 5µm, 200 Å, 125 µm x 16 cm) using a Famos autosampler (LC Packings). Peptides were separated by reversed-phase chromatography using an Agilent 1100 binary pump with a 70-minutes gradient of 5-30% ACN (in 0.125% FA). Peptides were detected in a hybrid dual-cell quadrupole linear ion trap - orbitrap mass spectrometer (LTQ Orbitrap Velos, ThermoFisher) using a data-dependent Top20 method (*8*). For each cycle, one full MS scan in the Orbitrap at 10^6 AGC target was followed by up to 20 MS/MS in the LTQ for the most intense ions. Selected ions were excluded from further analysis for 30 seconds. Ions with charge 1+ or unassigned were also rejected. Maximum ion accumulation times were 1000ms for each full MS scan and 150ms for MS/MS scans.

Database Searches and Peptide Quantification: Following acquisition of mass spectrometry data, RAW files were converted into mzXML format and processed with comprehensive proteomics data analysis software developed in-house. Individual precursors selected for MS/MS fragmentation were checked using algorithms that find and adjust incorrect monoisotopic peak assignments while refining precursor ion mass measurements. MS/MS spectra were searched against a composite database containing the mouse International Protein Index (IPI) database (*9*) and reversed 'decoy' versions of these proteins using the SEQUEST algorithm (*10, 11*). Peptide quantification was performed using the VISTA algorithm (*12*).

References cited in Supporting Information

1. **Mukherjee A, Sidis Y, Mahan A, Raher M, Xia Y, Rosen E, Bloch KD, Thomas MK, Schneyer AL** 2007 FSTL3 deletion reveals roles for TGFβ family ligands in glucose and fat homeostasis in adults. Proc Natl Acad Sci USA 104: 1348-1353.

2. **Mayhew TM, Olsen DR** 1991 Magnetic resonance imaging (MRI) and model-free estimates of brain volume determined using the Cavalieri principle. J Anat 178: 133-144.

3. **Wreford NG** 1995 Theory and practice of stereological techniques applied to the estimation of cell number and nuclear volume in the testis. Microsc Res Tech 32: 423-436.

4. **Baker PJ, O'Shaughnessy PJ** 2001 Role of gonadotrophins in regulating numbers of Leydig and Sertoli cells during fetal and postnatal development in mice. Reproduction 122: 227-234.

5. **Bastow ER, Lamb KJ, Lewthwaite JC, Osborne AC, Kavanagh E, Wheeler-Jones CP, Pitsillides AA** 2005 Selective activation of the MEK-ERK pathway is regulated by mechanical stimuli in forming joints and promotes pericellular matrix formation. J Biol Chem 280: 11749-11758.

6. **Coultas L, Bouillet P, Loveland KL, Meachem S, Perlman H, Adams JM, Strasser A** 2005 Concomitant loss of proapoptotic BH3-only Bcl-2 antagonists Bik and Bim arrests spermatogenesis. EMBO J 24: 3963-3973.

7. **Tolonen AC, Haas W, Chilaka AC, Aach J, Gygi SP, Church GM** 2011 Proteome-wide systems analysis of a cellulosic biofuel-producing microbe. Mol Syst Biol 7:461.

8. **Haas W, Faherty BK, Gerber SA, Elias JE, Beausoleil SA, Bakalarski CE, Li X, Villén J, Gygi SP** 2006 Optimization and use of peptide mass measurement accuracy in shotgun proteomics. Mol Cell Proteomics 5: 1326-1337.

9. **Kersey PJ, Duarte J, Williams A, Karavidopoulou Y, Birney E, Apweiler R** 2004 The International Protein Index: an integrated database for proteomics experiments. Proteomics 4: 1985-1988.

10. **Eng JK, McCormack AL, Yates JR** 1994 An approach to correlate tandem mass spectral data of peptides with amino-acid-sequences in a protein database. J Am Soc Mass Spectrom 5: 976-989.

11. **Elias JE, Gibbons FD, King OD, Roth FP, Gygi SP** 2004 Intensity-based protein identification by machine learning from a library of tandem mass spectra. Nat Biotechnol 22: 214-219.

12. **Bakalarski CE, Elias JE, Villén J, Haas W, Gerber SA, Everley PA, Gygi SP** 2008 The impact of peptide abundance and dynamic range on stable-isotope-based quantitative proteomic analyses. J Proteome Res 7: 4756-4765.

Supplemental Material

Supplemental Figure Legends

Supplemental Fig. 1: Genes differentially expressed during postnatal testis development. Genes in WT testes showing significantly increased expression in each of three age windows during postnatal testicular development, compared to the other two age groups tested. Cellular changes within the testis corresponding to these ages are presented as a schematic diagram on the left of the table. *Igfbp3* and *Igfbp5*, shown in bold, are amongst genes induced during the somatic cell expansion stage (0-14d) and are discussed in the main text.

Supplemental Fig. 2: AKT-mediated GSK3β phosphorylation and β-catenin expression is increased in FSTL3 KO testes. Western blot analyses of lysates from WT and FSTL3 KO testes showing (**A**) phospho-GSK3β and GSK3β (Mr: 46 kDa) and (**C**) β-catenin (Mr: 92 kDa) and tubulin (Mr: 65 kDa), as indicated. Densitometric analyses of Western blots showing the ratio of (**B**) phosphorylated to total GSK3β and (**D**) β-catenin to tubulin in WT and KO testes presented as bar graphs. (n = 3, error bars = SEM, ** = $p<0.001$).

Supplemental Fig. 3: Reduced apoptosis in FSTL3 KO testes. Representative TUNEL staining of apoptotic nuclei in WT and FSTL3 KO testes at 16 months. TUNEL positive nuclei are indicated by arrows. (Images are at 10x magnification)

Supplemental Fig. 4: SMAD2 activation is altered in FSTL3 KO testes. A: Immunostaining for phospho-SMAD2 (pSMAD2) in testicular sections from 4 month old WT and FSTL3 KO (KO) mice shown at 20x magnification. **B:** Microdensitometric

measurement of immunostaining obtained using phospho-SMAD2 antibody in the early (E) and late (L) cells of seminiferous tubules in testicular sections from WT and FSTL3 KO (KO) mice. **C:** Number of seminiferous tubules, shown as bar-graphs of the percentage of total tubules counted, that show no immunostaining (N), staining only in the early (E) or including late (L) spermatogenic cells using phospho-SMAD2 (pSMAD2) or phospho-SMAD5 (pSMAD5) antibodies in WT and FSTL3 KO testes. **D:** Examples of tubules classified as N, E and L. (Error bars = SEM, * = $p<0.05$).

Supplemental Fig. 5: Model depicting putative role of FSTL3 in testicular aging. Activin action promotes the maintenance of testicular function. FSTL3 inhibits activin action by directly binding to activin. In the absence of FSTL3, therefore, activin action is increased. In FSTL3 KO mice, AKT dependent signaling is also induced, either via increased activin action or indirectly, as a result of the removal of another inhibitory function of FSTL3. In the FSTL3 KO mice, therefore, AKT action-dependent cell survival mechanisms are induced: AKT-mediated phosphorylation and thus inhibition of GSK3β increases β-catenin, a promoter of cell growth, and AKT-mediated zyxin phosphorylation inhibits acinus, a promoter of cell apoptosis. An interaction partner for zyxin action is SIRT1. Both zyxin and SIRT1 are induced in FSTL3 KO testis possibly in an activin-induced SMAD-dependent manner. SIRT1 action might therefore contribute to anti-aging effects thus prolonging testicular function in the FSTL3 KO mouse. Green arrows denote stimulation, red lines denote inhibition and dotted lines signify postulated regulation.

Supplemental Table 1: Summary of candidate proteins important in maintenance of testicular size or age-related regression. List of proteins reduced or induced by at least 1.5 fold over WT with mean fold expression > 3SD.

Supplemental Table 1

	Fold change	Protein ID	MGI Gene Name
Reduced	58.43	IPI00604969	*Ttn*
	2.00	IPI00118438	*Srrm1*
	1.89	IPI00230124	*Fabp3*
	1.61	IPI00309964	*Nnt*
	1.53	IPI00132799	*C1qbp*
	1.50	IPI00125515	*Stard10*
Induced	3.14	IPI00170084	*2900057D21Rik*
	2.19	IPI00125319	*Gsk3b*
	2.11	IPI00113726	*Lama1*
	1.97	IPI00137908	*Col4a4*
	1.90	IPI00121430	*Col12a1*
	1.83	IPI00322304	*Hrg*
	1.81	IPI00128076	*Serpina3c*
	1.69	IPI00381431	*Xmr*
	1.68	IPI00315452	*Pnp*
	1.66	IPI00109588	*Col4a1*
	1.58	IPI00387422	*Zyx*
	1.54	IPI00114944	*BC003940*
	1.54	IPI00323822	*Rras2*
	1.52	IPI00341314	*Mdn1*
	1.52	IPI00230035	*Ddx3x*

Supplemental Fig. 1

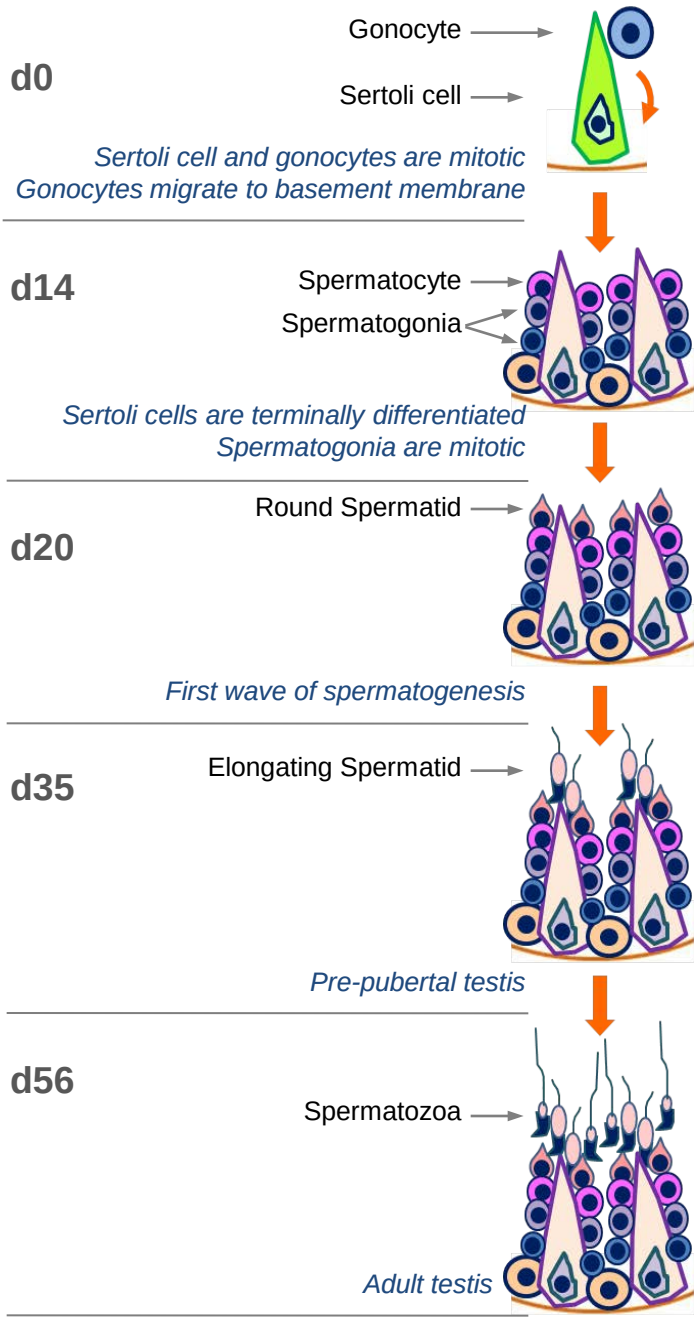

Age Group (days)	Genes Upregulated
0 -14	*Agtr2, Akap11, Art3, Bnc1, Bsg, Crabp1, Cul3, Ddx4, Dmc1, Dmrt1, Hmgn2, Hsdl2,* ***Igfbp3, Igfbp5****, Lox, Mest, Mns1, Nefh, Nono, Nptx2, Pick1, Pno1, Smo, Sox18, Srpk1, Srpk2, Tbl2, Tgfbr3, Trim37, Ube1y1, Vnn1*
20 - 35	*Cd34, Cetn1, Cftr, Dcn, Dhh, Dnajb6, Galt, Gas8, Inpp5b, Lama4, Nkx3-1, Psme4, Ptn, Rbm3, Rbmx, Sfpq, Sh3gl1, Smad7, Tdg, Zfp105*
20 - 56	*Acrbp, Adipor2, Cdk4, Dnajb13, Fabp9, Gnas, Gnpat, Hsp90ab1, Islr, Meig1, Mgp, Nphp1, Pdgfra, Prdx6, Psmd6, Rad51, Reep1, Rnf19a, Slc11a2, Sp4, Sparc, Thra, Usp2*

Supplemental Fig. 2

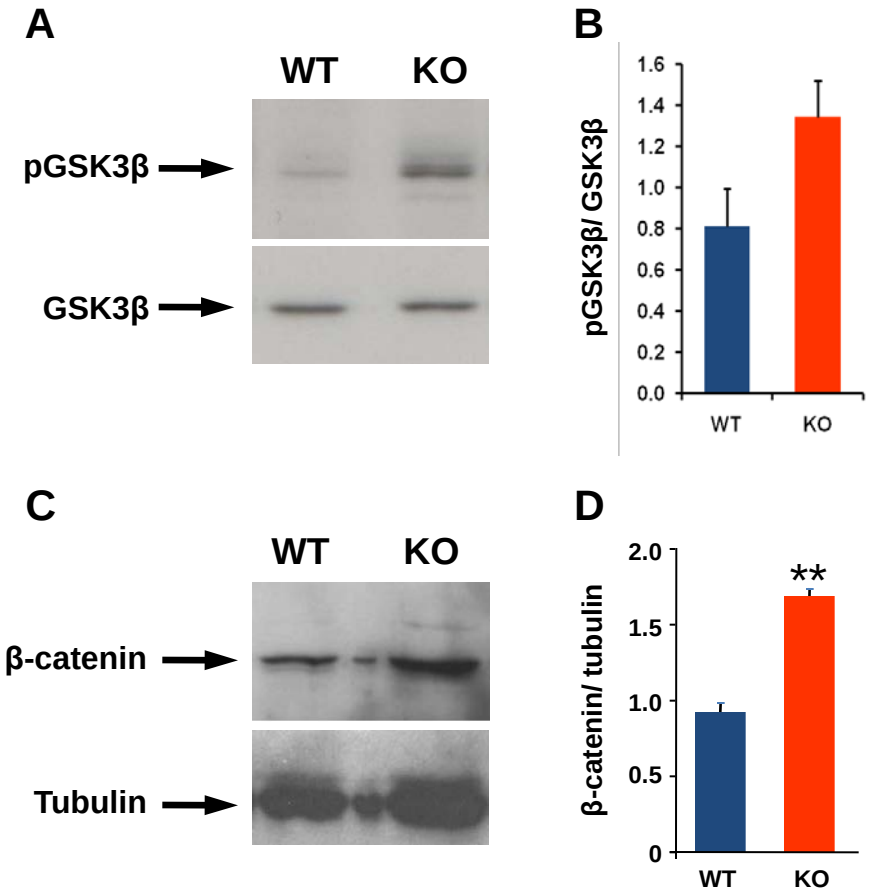

Supplemental Fig. 3

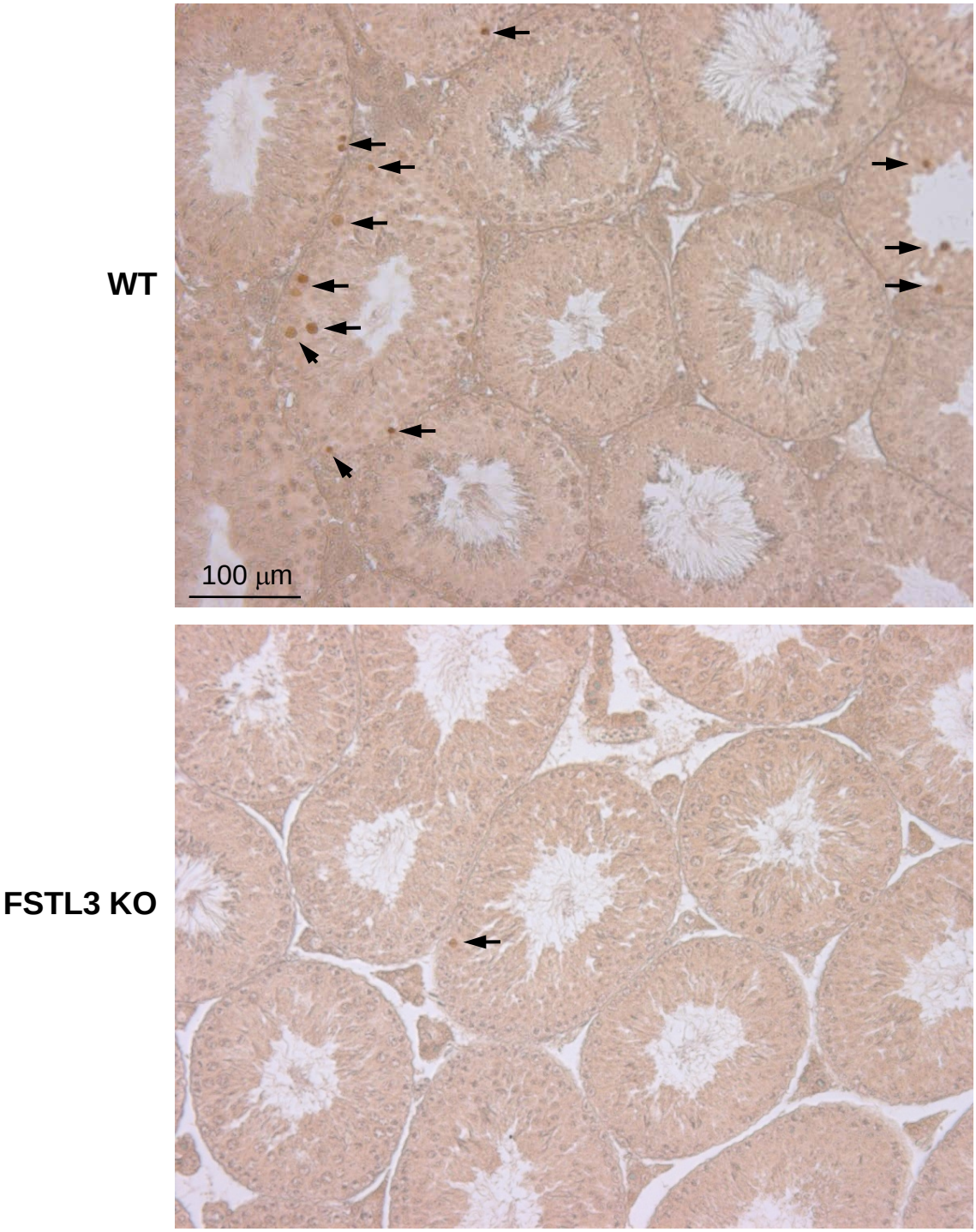

Supplemental Fig. 4

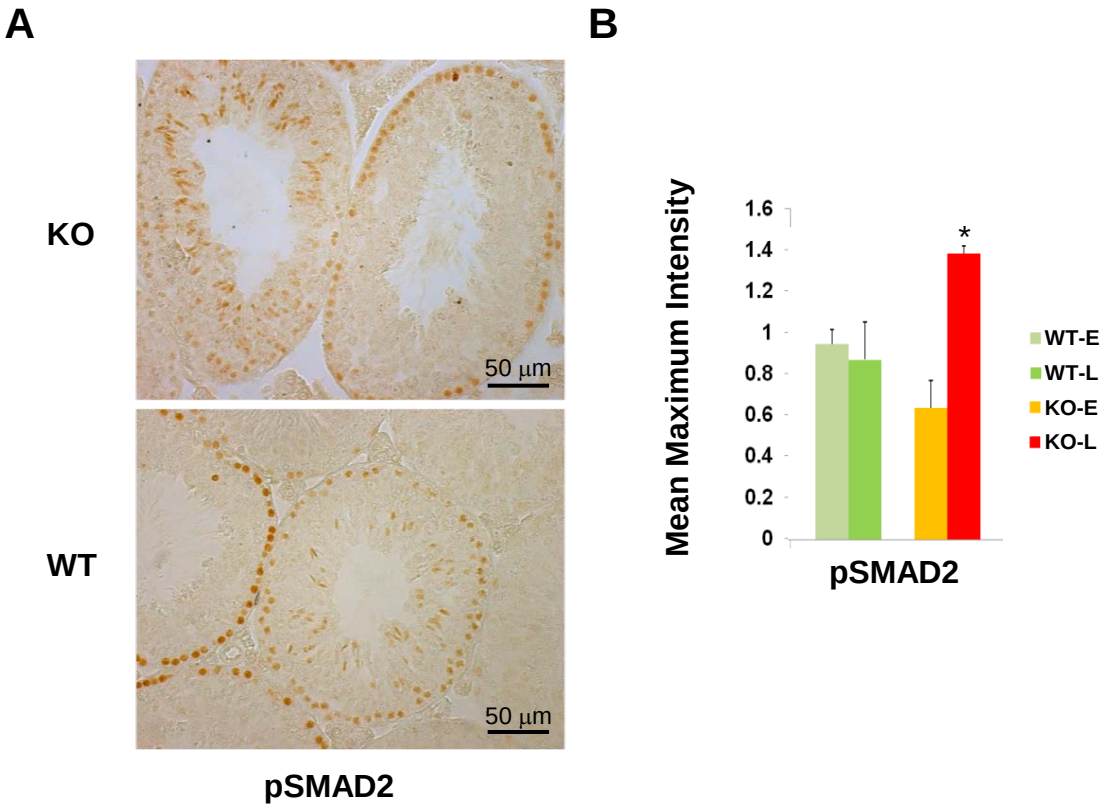

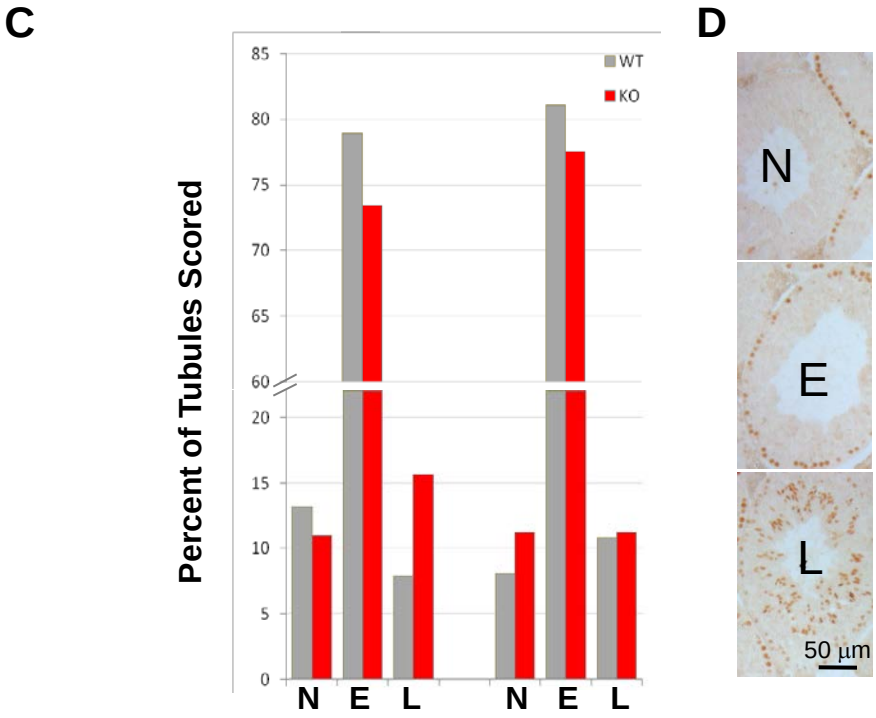

Supplemental Fig. 5